Journal of Thermal Analysis, Vol. 42 (1994) 1193-1205

CONDUCTION MECHANISMS OF ANTIMONY SELENIDE

M. M. Ibrahim, M. M. Wakkad and E. Kh. Shokr

Physics Department, Faculty of Science, Sohag, Egypt

(Received April 3, 1993; in revised form September 15, 1993)

Abstract

The electrical resistivity, ρ, and Seebeck coefficient, S, of the system Sb_2Se_3 were measured in the ambient temperature range $323 \leq T \leq 573$ K. Both parameters were found to be affected considerably by the temperature of annealing, T_a, in the range $493 \leq T_a \leq 653$ K and by the time of annealing, t_a, for periods extending to 16 h. Additionally, both depended strongly on the ambient temperature.

The activation energy of ordering of the present system could be calculated by using the effects of isothermal annealing on the considered physical parameters.

Keywords: antimony selenide, conduction mechanism, kinetics

Introduction

In recent years, considerable attention has been focused on glasses of Sb and Se because of their switching characteristics [1, 2]. As concerns optical and transport studies of these glasses, Wood *et al.* [2] pointed out that addition of Sb to amorphous Se reduces the S_8 ring concentration and leads to the formation of branched Se chains. They also have found a peak at Sb_2Se_3 in the optical and thermal activation energy versus composition curves. Their results suggested that an ordering into molecular units corresponding to crystalline Sb_2Se_3 is present in the amorphous phase. The photoemission study by Hurych *et al.* [3] suggested that amorphous Sb_2Se_3 is a random aggregate of Sb_4Se_6 molecules.

Investigations [4] of the static current-voltage characteristics of Sb_2Se_3–Bi_2Se_3 alloys, which form a continuous series of solid solutions [5, 6], revealed several features indicative of switching from a high-resistivity to a low-resistivity state. The investigations were carried out on polycrystalline and single-crystal samples. The results confirmed that the current-voltage characteristics of Sb_2Se_3 and of alloys containing more than 50 wt% Sb_2Se_3 are linear up to 20–40 V (depending on the composition). At higher voltages, the dependence

0368–4466/94/ $ 4.00

John Wiley & Sons, Limited
Chichester

of the characteristics becomes sublinear. At 80–100 V, the current rises suddenly and the voltage falls to some minimum value, at which the characteristic exhibits a vertical section. At the same time, the temperature of the sample rises considerably.

Tatarinova [7] analysed the amorphous phase of Sb_2Se_3 by the electron diffraction method. The results indicated that the interatomic distance for amorphous Sb_2Se_3 is much less than that for the crystal, and the coordination number increases considerably in the amorphous phase.

The present work investigates the effects of the temperature and time of annealing on the electrical resistivity and Seebeck coefficient of Sb_2Se_3 in an attempt to identify the conduction mechanism. Isothermal annealing methods are also considered, to calculate the activation energy of ordering.

Experimental technique

The preparation of the required specimens, the techniques and the measurement procedures were basically as described elsewhere [8, 9]. Very briefly, appropriate amounts of Sb and Se (99.999% purity) were charged in a quartz ampoule, sealed off at 10^{-5} Torr and melted at about 1073 K for about 24 h. The ampoules were occasionally agitated by rocking to ensure homogeneity of the melt. The melt was then quenched in ice-water. The X-ray diffraction (XRD) patterns obtained (using a Philips PW 1710 X-ray diffractometer) proved that this method results in the preparation of polycrystalline specimens.

The electrical resistivity measurements were carried out by applying a known potential difference across a disk-shaped sample 1 cm in diameter and 0.4 cm thick and measuring the series current passing through it. The series current was measured by using a Gould advance Beta digital multimeter (sensitivity 1 μA) and the potential difference across the specimen was measured by means of a Keithley 191 digital multimeter (sensitivity 1 μV)

Seebeck coefficient measurements were made in the conventional manner by keeping the temperature difference, ΔT, between the opposite surfaces of the specimen at about 5 deg. The junctions of two copper-constantan thermocouples conducted well at both surfaces of the specimen. The temperature difference was determined by measuring separately the thermovoltages of both thermocouples by means of a Keithley 191 digital multimeter. The generated thermoelectric power, TEP, was measured over the copper wires by means of a Keithley 614 digital electrometer (sensitivity 10 μV) and was corrected for the absolute thermovoltage of the copper [10].

In the present study, the specimens were annealed at different annealing temperatures in the range $493 \leq T_a \leq 653$ K for periods extending to 16 h. The electrical resistivity and Seebeck coefficient were measured at various tempera-

tures in the range $323 \leq T \leq 573$ K, the starting temperature being that of the room.

Results and discussion

X-ray diffraction examinations

Figure 1 shows the X-ray diffraction patterns of as-prepared and of annealed (at T_a = 613 K for t_a = 16 h) specimens of Sb_2Se_3 alloy. Tables 1a and b list the corresponding X-ray parameters for the as-prepared and the annealed samples, respectively.

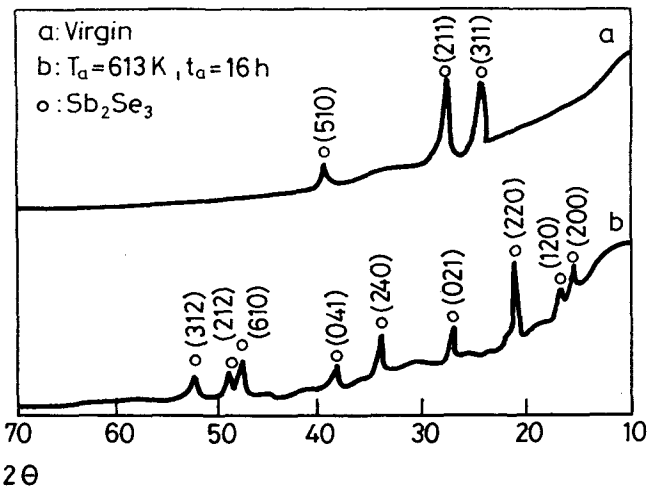

Fig. 1 X-ray diffractograms for specimens as-prepared or annealed at 613 K for 16 h

Table 1a X-ray parameters of as-prepared Sb_2Se_3 alloy

d–spacing / Å	3.57	3.17	2.26
I/I_o	95.2	100	35.2
h k l	3 1 0	2 1 1	5 1 0

Table 1b X-ray parameters of annealed Sb_2Se_3 alloy (at T_a = 613 K for t_a = 16 h)

d–spacing / Å	5.74	5.39	4.19	3.29	2.64	2.36	1.90	1.86	1.75
I/I_o	96.2	81	100	54.4	48.1	27.9	32.9	22.8	21.5
h k l	2 0 0	1 2 0	2 2 0	0 2 1	2 4 0	0 4 1	6 1 0	2 1 2	3 1 2

All the peaks that appeared in the diffractograms and are recorded in the two tables correspond to the same Sb_2Se_3 phase [11]. Therefore, it could be concluded that:

1. the disappearance of the elemental phases of both Sb and Se ensures that the method used leads to good alloying;
2. the disappearance of the present peaks for the as-prepared sample and the appearance of new peaks on annealing indicates that the process of annealing can result in more ordering, which is associated with different orientations of the already existing Sb_2Se_3 crystallites.

Effect of annealing temperature

The Sb_2Se_3 specimens were annealed at different annealing temperatures in the range $493 \leq T_a \leq 653$ K for periods extending to 16 h. The electrical resis-

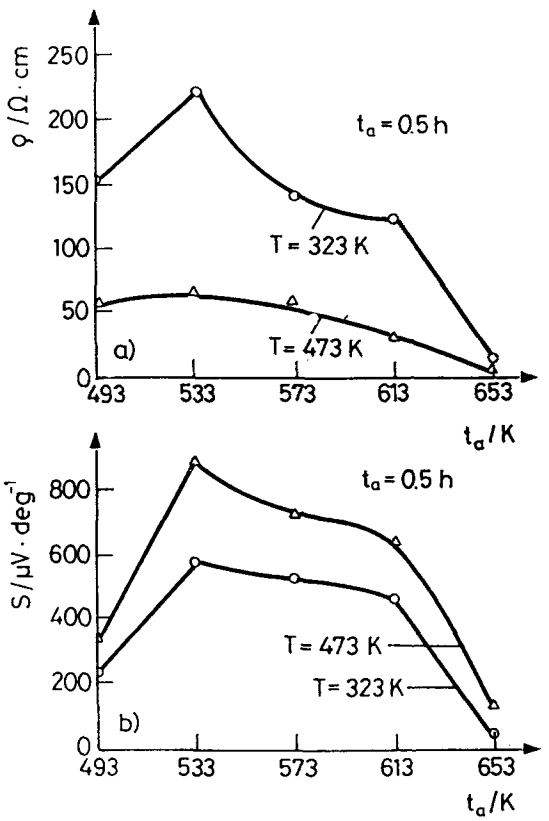

Fig. 2 Dependence of (a) electrical resistivity and (b) Seebeck coefficient on annealing temperature; t_a = 0.5 h

tivity and Seebeck coefficient were measured in the range $323 \leq T \leq 573$ K after the specimens had cooled to room temperature.

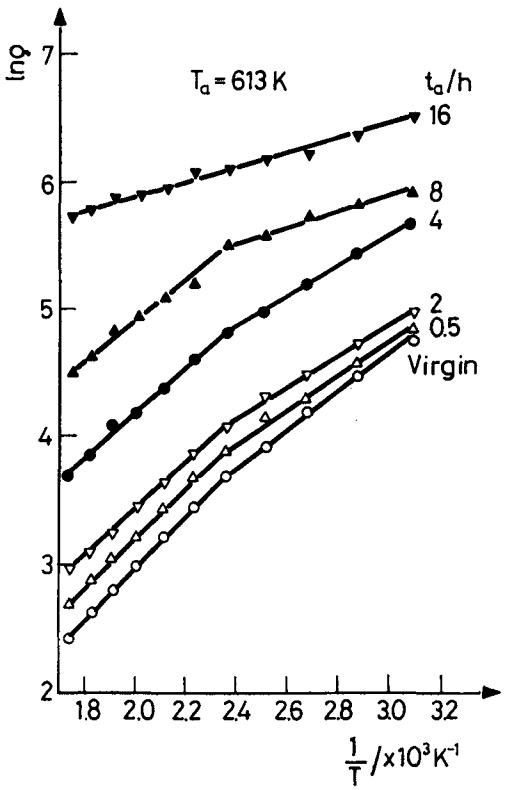

Fig. 3 ln ρ *vs.* $1/T$ dependence for specimens as-prepared or annealed at 613 K for different periods of time

Figures 2a and b show the variations with annealing temperature in ρ and S (measured at T = 323 and 473 K) for specimens annealed for 30 min. In the range $T_a \leq 533$ K, both ρ and S increased, maxima being attained at 533 K. Further increase of T_a was associated with a continuous decrease in both ρ and S. This behaviour might suggest that the conduction is mixed; i.e. a mechanism involving two charge carriers can be considered to explain the variations in ρ and S with T_a. As both electrons and holes contribute to conduction, the activation of holes is predominant, since the sign of S was positive over the whole range considered for T_a. However, this is behaviour characteristic of most chalcogenide [12]. The observed increases in ρ and S in the range $T_a \leq 533$ K can be explained on the basis that, when the concentration of holes is still fixed, the

concentration of electrons is expected to decrease. This is a consequence of two contributions:

(i) the lower compensation of the holes, which results in an increase in the positive sign S;

(ii) a reduction of the total charge concentration, which results in a resistivity increase.

In the range $T_a \geq 533$ K, the concentration of the contributing electrons is expected to increase at the expense of that of the holes. This can result in a greater compensation of the holes, which results in turn in a decrease in the positive S. On the other hand, considering that hopping and extended band conduction mechanisms contribute together, elevation of the temperature of annealing can result in a greater predominance of extended band type conduction. This can result in an increase in the observed conductivity, i.e. a decrease in the resistivity, which is the case.

The increases in both $1/\rho$ and S on increase of the ambient temperature from 323 to 473 K at all considered annealing temperatures, as shown in Figs 2a and b may be due to the fact that the mobility is thermally activated and the principal charge carriers of the considered system become more mobile with increasing temperature.

Effect of ambient temperature

The temperature dependences of ρ and S were studied for samples annealed at 613 K for different periods of time extending to 16 h. The annealing temperature of 613 K was chosen because it lies at the mid-value of both ρ and S, as shown in Fig. 2. This might indicate the temperature at which the effects of the decreases in the density of the band tail and the centre of the defects are equilibrated.

As shown in Fig. 3, the plots of ln ρ *vs.* $1/T$ are kinked linear, showing two regions corresponding to the high- and low-temperature ranges. Each verifies the Arrhenius relationship for the resistivity *vs.* temperature dependence [13]:

$$\rho = \rho_o \exp (E_\rho/kT) \quad (1)$$

where E_ρ is the activation energy for conductivity, k is Boltzmann's constant and ρ_o is a preexponential factor (or the temperature-independent resistivity), which is equal to $1/e\mu N_v$ [14], where μ and N_v are the mobility and the effective density of states in the valence band, respectively.

Figure 4 shows plots of the Seebeck coefficient *vs.* $1/T$ for a specimen annealed at 613 K for periods extending to 16 h. This figure reveals that this sys-

tem exhibits a positive thermoelectric power, which is the behaviour of *p*-type semiconductors. Further, the *S vs.* $1/T$ plots possessed negative slopes, similarly as expected for degenerate semiconductors [12]. As shown in Fig. 4, each *S vs.* $1/T$ plot seems to consist of two linear segments satisfying the following relation:

$$S = \frac{k}{e}\left(\frac{E_s}{kT} + A'\right) \tag{2}$$

where E_s is the activation energy of thermoelectric power and A' is a parameter relating to the carrier scattering mechanisms and assumed to be unity for amorphous semiconductors [15]. As an alternative option in standard thermopower theory [16], the parameter A' is assumed to be a measure of the kinetic energy transported by the carriers and is positive. Both E_s and A' were calculated and are recorded in Table 2.

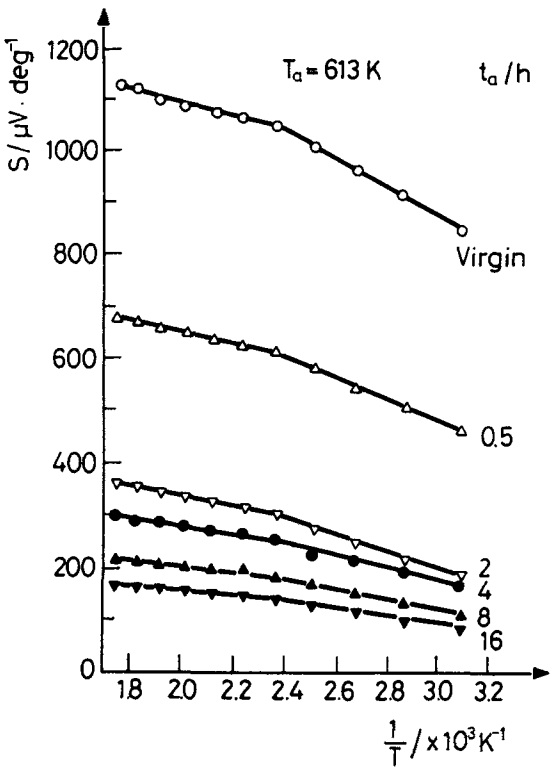

Fig. 4 *S vs.* $1/T$ dependence for specimens as-prepared or annealed at 613 K for different periods of time

Table 2 Variation in activation energies of conduction and thermoelectric power at low temperatures ($E_{\rho 1}$ and E_{s1}) and high temperatures ($E_{\rho 2}$ and E_{s2}) and of parameters ρ_o and A' with time of annealing; T_a = 613 K

t_a / h	$E_{\rho 1}$ / eV	$E_{\rho 2}$ / eV	ρ_o / Ω·cm	E_{s1} / eV	E_{s2} / eV	A'
Virgin	0.127	0.174	0.347	0.272	0.128	15.67
0.5	0.108	0.168	0.499	0.205	0.113	10.17
2	0.101	0.160	0.752	0.164	0.097	6.21
4	0.099	0.158	1.134	0.124	0.061	4.71
8	0.049	0.134	5.930	0.101	0.051	3.54
16	0.047	0.055	102.524	0.073	0.034	2.66

The data in Figs 3 and 4 and Table 2 permit certain conclusions:

1. The electrical resistivity increases with the time of annealing. This may be attributed to a decrease in the effective density of states in the valence band, N_v. However, it is acceptable since ρ_o increases with prolongation of t_a, as shown in Table 2 on considering the constancy of the charge carrier mobility.

2. In both ranges of ambient temperatures and for all conditions considered for annealing, the activation energies calculated from electrical and TEP measurements are not equal. However, the results indicate that $E_{s1} > E_{\rho 1}$, while $E_{s2} < E_{\rho 2}$. According to [17–19] for germanium chalcogenide systems, three different models have been proposed to explain the inconsistency in the values of E_ρ and E_s. These are:

(i) two-carrier conduction,

(ii) one-carrier conduction with thermally activated mobility, and

(iii) a two-channel conduction model where the conduction occurs through both the extended states and hopping through the tail of localized states.

For the present system, the variations in both ρ and S with the ambient temperature indicate that the first model can explain the obtained results, especially in the relatively low range of T. As concerns the two-carrier conduction mechanism, the positivity of S proves that holes predominantly contribute to the observed increase in S and the decrease in ρ with increase of the ambient temperature. On the other hand, the hole concentration is more thermally activated and matches the activation of mobility in the relatively low range of T. This can explain why $E_{s1} > E_{\rho 1}$. In the successive high range of T, the contribution of electrons to the conduction becomes appreciable. Thus, a greater compensation of the positive holes can be observed. This will result in a relatively slow change in S, which is characterized by relatively small values for E_{s2}

with respect to E_{s1}. This appreciable contribution of electrons contributes to an appreciable increase is the conductivity, which can be revealed through the fact that $E_{\rho 1} < E_{\rho 2}$ and thus $E_{s2} < E_{s1}$. However, as discussed earlier, when it is considered that both hopping and extended state conduction mechanisms contribute, the latter becomes more predominant as T exceeds a certain value characterizing the transition between the two observed ranges of dependence of both S and ρ on T.

3. The values of E_ρ and E_s both decreased on increase of the time of annealing. This may be due to the decrease in disordering of the considered alloy on heat treatment, which could be proved by X-ray analysis.

4. The values of ρ_o increased on increase of the time of annealing. This may reflect the possibility of decreases in the effective density of the states and/or inhibition of the mobility with the annealing time.

5. The parameter A' decreased on increase of the time of annealing. This may be associated with a corresponding decrease in the charge carrier concentration as a result of the decrease in the effective density of the states with the time of annealing. As for ρ_o, the inhibition of mobility due to scattering can play a significant role.

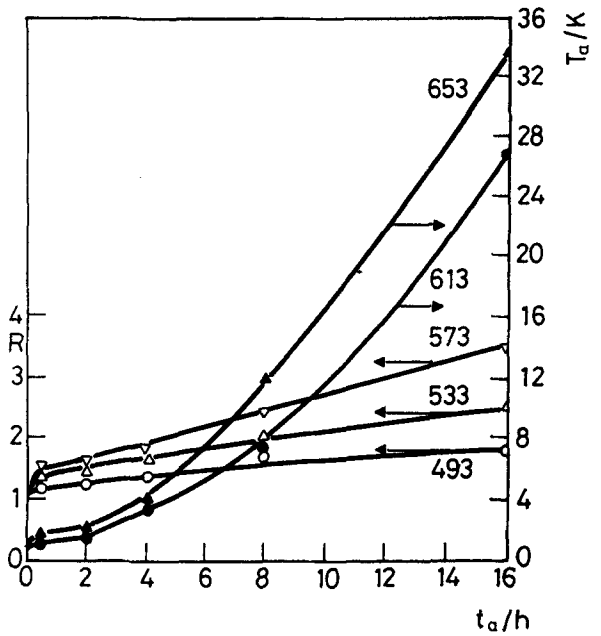

Fig. 5 *R vs.* t_a dependence for specimens annealed at different temperatures

Activation energy of ordering

According to [20], the local method for calculating the activation energy of ordering is used and so the following equation should be considered:

$$\ln \left| \frac{dR}{dt_a} \right|_{max} = - \frac{E_{op}}{kT_a} + const. \quad (3)$$

where $|dR/dt_a|_{max}$ is the maximum of the absolute value of the first time derivative of the reduced electrical resistivity R (defined as the actual electrical resistivity divided by its room temperature value).

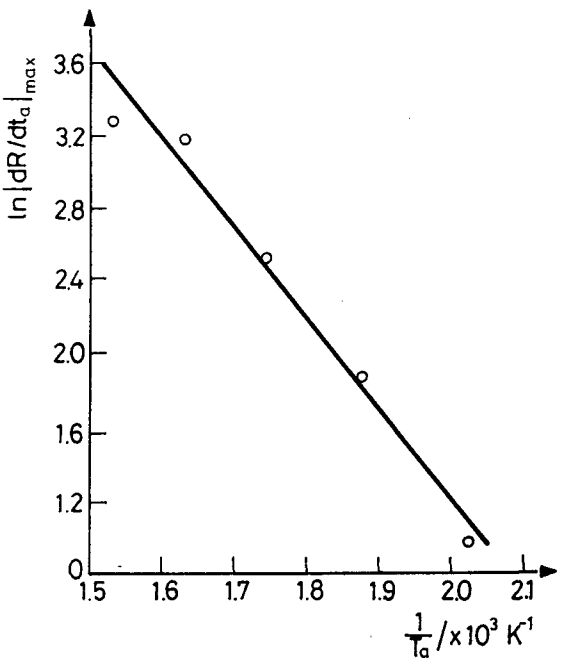

Fig. 6 $\ln |dR/dt_a|_{max}$ *vs.* $1/T_a$ dependence for specimens annealed at different temperatures

Figure 5 shows the dependence of the reduced electrical resistivity on the time of annealing for different specimens annealed at different temperatures in the range $493 \leq T_a \leq 653$ K. However, because of the high sensitivity of R to the annealing temperature, two different scales were used on the ordinate of Fig. 5 for graphical presentation of the change in R with the time of annealing. Thus, values of $|dR/dt_a|_{max}$ can be obtained. Hence, as shown in Fig. 6, the dependence of $\ln |dR/dt_a|_{max}$ on the reciprocal of the temperature of annealing in Kelvin is drawn. Plots of this type are linear, with a slope coefficient equal to

$-E_{op}/k$ (Eq. (3)) and correlation coefficient equal to 0.9873. The value of the activation energy of ordering, E_{op}, of the present system was calculated by using least square fitting. It was equal to 0.42 eV.

On the same basis [20] of deriving Eq. (3), the following equation could be derived for the dependence of $|dS'/dt_a|_{max}$ on the temperature of annealing:

$$\ln \left| \frac{dS'}{dt_a} \right|_{max} = -\frac{E_{os}}{kT_a} + const. \quad (3')$$

where $|dS'/dt_a|_{max}$ is the maximum absolute of the first time derivative of the reduced thermoelectric power, S' (defined as the actual thermoelectric power divided by its room temperature value). Figure 7 shows the dependence of S' on the time of annealing for specimens annealed at different annealing temperatures in the range $493 \leq T_a \leq 653$ K.

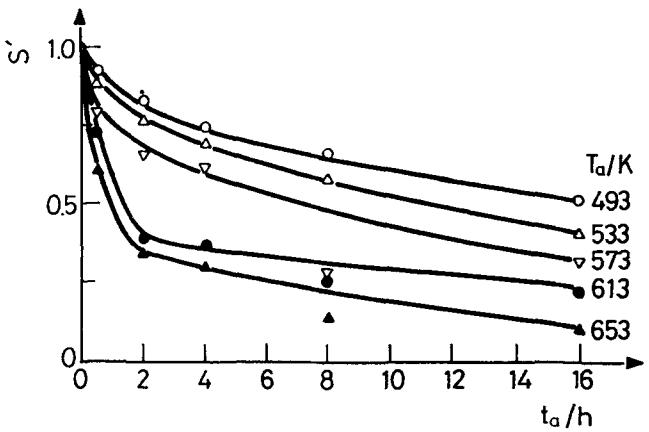

Fig. 7 S' *vs.* t_a dependence for specimens annealed at different temperatures

From this figure, the values of $|dS'/dt_a|_{max}$ can be deduced at all considered annealing temperatures. In the second step, obtained values of $\ln |dS'/dt_a|_{max}$ are plotted *vs.* the reciprocal of the temperature of annealing. As shown in Fig. 8, the plots are linear, with a correlation coefficient equal to 0.9848. The value of the activation energy of ordering, E_{os}, obtained from these results by using least square fitting was found to be equal to 0.27 eV.

Conclusions

Thermal annealing has significant effects on the microstructure and ordering of the present system, as proved by X-ray diffraction examination.

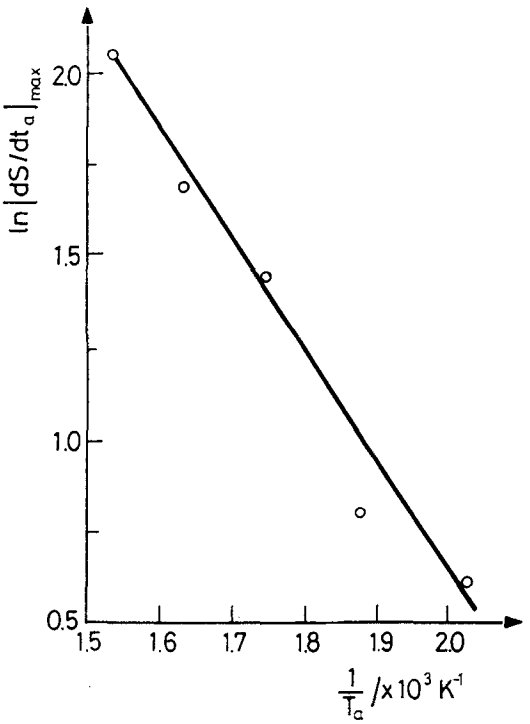

Fig. 8 $\ln \left| dS'/dt_a \right|_{max}$ *vs.* $1/T_a$ dependence for specimens annealed at different temperatures

The change in the microstructure of the present system on thermal annealing is responsible for the observed variations in both electrical resistivity and Seebeck coefficient, which can reflect the variations in the parameters E_p, ρ_o, E_s and A' with variation of the conditions of annealing.

Isothermal annealing studies on both ρ and S gave a possibility to calculate the activation energy of ordering, equal to 0.42 and 0.27 eV, respectively.

References

1 S. Luby, J. Cervenak, J. Kubek, M. Marcin and J. Schilder, Czech. J. Phys., B 21 (1971) 878.
2 C. Wood, R. Mueller and L. R. Gilbert, J. Non-Cryst. Solids, 12 (1973) 295.
3 Z. Hurych, R. Mueller, C. C. Wang and C. Wood, J. Non-Cryst. Solids, 11 (1972) 153.
4 L. G. Gibnyak, Soviet Physics-Semiconductors, 6 (1972) 478.
5 N. M. Bondar, Neorg. Mater., 2 (1966) 1144, (in Russian).
6 L. G. Gibnyak and N. M. Bondar, Ukr. Fiz. Zh., 4 (1969) 1223, (in Russian).
7 L. I. Tatarinova, Kristallografiya, 4 (1959) 678.

8 M. M. Ibrahim, N. Afifi, M. M. Hafiz and M. A. Mahmoud, Powder Metallurgy International, 20 (1988) 21.
9 M. M. Ibrahim, E. Kh. Shokr, M. M. Wakkad and N. M. Megahid, Bulletin of Faculty of Science, Assiut University, Assiut, Egypt, 17 (1988) 123.
10 Y. R. Shen, W. F. Leonard and H. Y. Yu, Rev. Sci. Instrum., 48 (1977) 688.
11 Natl. Bur. Stds. U.S. Mono., 25 (1964) Sec. 37.
12 H. K. Rockstad, R. Flasck and S. Iwasa, J. Non-Cryst. Solids, 8–10 (1972) 326.
13 R. Kassing and W. Bax, Jpn. J. Appl. Phys. 13 (1974) 801.
14 N. Tohge, T. Minami and M. Tanaka, Jpn. J. Appl. Phys., 16 (1977) 977.
15 N. F. Mott and E. A. Davis: Electronic Processes in Non-Crystalline Materials, Clarendon Press, Oxford 1977, p. 217.
16 A. F. Ioffe, Physics of Semiconductors, Infosearch, London 1960, p. 288; R. R. Heikes and R. W. Ure, Jr., Thermoelectricity: Science and Engineering, Intersicence, New York 1961; J. Tauck, Photo and Thermoelectric Effects in Semiconductors, Pergamon, New York 1962.
17 N. Tohge, T. Minami and M. Tanaka, J. Non-Cryst. Solids 37 (1980) 23.
18 N. F. Mott, E. A. Davis and R. A. Street, Phil. Mag., 32 (1975) 961.
19 P. Nagels, R. Callerts and M. Denayer, Amorphous and Liquid Semiconductors, Edited by J. Stuke and W. Brenig, Taylor and Francis Ltd., London 1974, p. 867.
20 J. Wolny, R. Kokozka, J. Soltys and P. Barta, J. Non-Cryst. Solids, 113 (1989) 171.

Zusammenfassung — In einem Umgebungstemperaturbereich von 323 bis 573 K wurden der elektrische Widerstand ρ und der Seebock'sche Koeffizient S des Systemes Sb_2Se_3 untersucht. Für beide Größen wurde eine starke Abhängigkeit von der Tempertemperatur T_a im Bereich $493 \leq T_a \leq 653$°C und von der Temperdauer t_a bis zu 16 Stunden beobachtet. Zusätzlich sind beide auch stark abhängig von der Umgebungstemperatur.
Unter Ausnutzung der Auswirkung des isothermen Temperns auf die fraglichen physikalischen Größen konnte die Aktivierungsenergie der Konditionierung berechnet werden.